



Analysis and Optimization of Cogging Torque in Line-Start Permanent Magnet Synchronous Machine by Changing the Rotor Teeth and Slots

Jing He¹(✉), Ronaldo Juanatas²(✉), and Jin-lin Huang^{1,2}

¹ Anhui Technical College of Mechanical and Electrical Engineering, Wuhu 241002, Anhui, China

0121000098@ahcme.edu.cn

² Technological University of the Philippines, Manila, Philippines

Abstract. When the windings of permanent magnet machine (PMM) are not energized, the interaction between the permanent magnet and the armature core generates cogging torque. It will cause vibration, noise and speed fluctuation. As for line-start PMM, both the stator and rotor core are slotted, and the manufacturing tolerances have influenced on cogging torque. The analytical expression of cogging torque of line-start PMM is obtained by using the equivalent method of rotor permanent magnets magneto motive force (MMF). Based on the analytical expression, the influence of rotor slots processing technic, magnetic bridge manufacturing parameters as well as permanent magnets technology on cogging torque are analyzed. Furthermore, the optimum combination of these three factors is deduced to minimize the cogging torque of line-start PMM. The finite element method (FEM) calculation verifies that the proposed method can reduce the cogging torque of LSPMSM.

Keywords: Cogging torque · Manufacturing tolerances · Line-start PMSM · Optimization

1 Introduction

Self-starting permanent magnet synchronous motor (LSPMSM) is receiving more and more attention. The main reason is that, firstly, high-energy rare earth permanent magnet (PM) materials can provide high air-gap magnetic flux density, thus reducing copper loss and providing high power factor [1]. At the same time, LSPMSM has the self-starting ability and high efficiency, making it more suitable for pump sets, compressors and some energy-saving applications [2, 3].

The interaction between the permanent magnet motor and the stator slot will occur when the motor is unloaded, resulting in cogging torque. It will cause vibration, noise and speed fluctuation. For linear starting PMM, the slot and tooth parameters of stator and rotor will have a great impact on the cogging torque [4, 5]. In order to reduce the cogging torque, the influence on of the cogging torque for stator tooth width have been studied in [6–8]. In [9], the cogging torque have been weakened by the unequal stator

tooth width. However, the above research is limited to single-side slotted PMM, and there is little literature on the analysis of cogging torque of line-start PMSM.

The stator slot and rotor slot are existed in LSPMSM, and the distribution of effective air-gap length is more complex compared with the traditional PMSM when the relative position of the stator and rotor is changed. The traditional method of reduce cogging torque cannot apply to the LSPMSM directly. The distribution of effective air-gap of LSPMSM is obtained through the superimposed the effective air-gap of the stator side and rotor side, and then the analytical expression of cogging torque is obtained in [10, 11]. In addition, the generation mechanism of LSPMSM cogging torque is discussed. However, the expression used to analyse the cogging torque is extremely complex [12, 13].

Based on the energy method and Fourier decomposition method, the analytical expression of cogging torque of linear starting permanent magnet synchronous motor is derived in this paper, including rotor slot offset angle, magnetic bridge as well as permanent magnets width. Based on the analysis above, the optimum combination of these three parameters are proposed to minimize cogging torque.

2 Analytical Model of Lspmsm Cogging Torque

According to the mechanism of cogging torque, and the cogging torque can be followed by:

$$T_{\text{cog}} = -\frac{\partial W}{\partial \alpha} \quad (1)$$

where W is magnetic field energy, and α is relative position angle of the stator and rotor.

Suppose the magnetic permeability of the rotor core is infinite, and the magnetic field energy in the stator and rotor core can be neglected compared with the magnetic field energy in the air-gap. Therefore, the magnetic field energy can be given by:

$$W \approx W_{\text{airgap}} = \frac{1}{2\mu_0} \int_V B^2(\theta, \alpha) dV \quad (2)$$

where μ_0 is the air permeability, $B(\theta, \alpha)$ is the distribution of air-gap flux density along the circumferential direction as the position of the stator and rotor changes.

Here, the distribution of air-gap flux density can be followed by:

$$B(\theta, \alpha) = \mu_0 \frac{F(\theta)}{\delta(\theta, \alpha)} \quad (3)$$

where $\delta(\theta, \alpha)$ is the effective air-gap length of versus the position of stator and rotor core.

There are many kinds of magnetic circuit structures of LSPMSM, and the interior structure can improve the power density. Figure 1 shows the configuration of spoke-type LSPMSM. It can be seen that the structure is different from the traditional permanent magnet synchronous machines (PMSMs). Due to the rotor slot is existed in LSPMSM rotor core, and the distribution of effective air-gap length is more complex compared

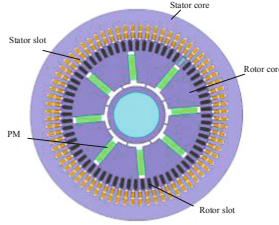


Fig. 1. Relative position of the stator and rotor

with traditional PMSMs. In order to reduce the difficulty of cogging torque analytical expression, and the rotor magnetomotive force (MMF) is represented by a distributed MMF.

Hence, the distribution of effective air-gap length is only related to the stator slots and teeth. The magnetic field energy can be followed by.

$$W \approx W_{\text{airgap}} = \frac{\mu_0}{2} \int_V F^2(\theta, \alpha) \frac{1}{\delta^2(\theta, \alpha)} dV \quad (4)$$

Furthermore, when the stator and rotor leakage flux is ignored, and the air-gap MMF $F(\theta)$ is produced rotor is shown in Fig. 2. As shown in Fig. 2, p is the pole pairs, τ_r is the distance of rotor tooth, θ_{rt} is the rotor tooth, F is the amplitude of air-gap MMF. As a result, the distribution map of $F^2(\theta)$ is shown in Fig. 3, and the Fourier expansion can be expressed as.

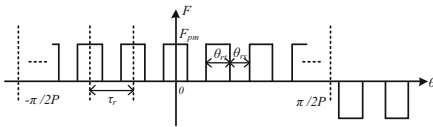


Fig. 2. Distribution of the equivalent MMF of rotor

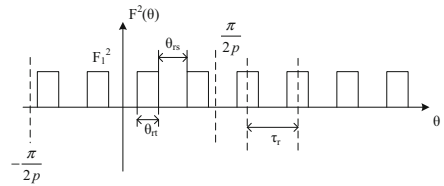


Fig. 3. Distribution of $F^2(\theta)$

$$F^2(\theta, \alpha) = F_0 + \sum_{n=1}^{\infty} F_n \cos 2np\theta \quad (5)$$

where, the Fourier decomposition coefficient F_0 can be expressed as

$$F_0 = \frac{(Q_2 - 1)pF^2}{\pi} \theta_{rt} \quad (6)$$

$$F_n = \begin{cases} (-1)^{n+1} \frac{2F_1^2}{n\pi} \sin np\theta_{ra}, & n \text{ is not an integer multiple of } Q_2 \\ (-1)^n \frac{2(Q_2-1)F_1^2}{n\pi} \sin np\theta_{ra}, & n \text{ is an integer multiple of } Q_2 \end{cases} \quad (7)$$

where Q_2 is number of rotor slots, p is pole paris.

Moreover, $\frac{1}{\delta^2(\theta, \alpha)}$ is only related to stator slot and tooth, and the Fourier expansion can be expressed as.

$$\frac{1}{\delta^2\theta} = G_0 + \sum_{n=1}^{\infty} G_n \cos nQ_1\theta \tag{8}$$

$$\frac{1}{\delta^2\theta, \alpha} = G_0 + \sum_{n=1}^{\infty} G_n \cos nQ_1(\theta + \alpha) \tag{9}$$

where Q_1 is number of stator slots, and the Fourier decomposition coefficient G_0 can be expressed as.

$$G_0 = \frac{Q_1 \tau_s}{2\pi \delta^2} \tag{10}$$

$$G_n = \frac{2}{n\pi \delta^2} \sin \frac{nQ_1 \tau_s}{2} \tag{11}$$

where τ_s is the stator tooth width.

At last, the LSPMSM cogging torque expression can be followed by.

$$T_{cog} = \frac{\pi Q_1 L_{Fe}}{4\mu_0} (R_2^2 - R_1^2) \sum_{n=1}^{\infty} n G_n B_r \frac{nQ_1}{Q_2} \sin nQ_1\alpha \tag{12}$$

where L_{fe} is the armature core axial length, R_1 is the outer radius of the rotor, and R_2 is the inner radius of the stator, n is an integer which $nQ_1/2p$ is integer.

According to the formula 12, the number of rotor slot, rotor tooth width, air-gap length, he tooth width and slot width of the stator will affect G_n and the amplitude of the cogging torque. Based on this, this paper studies these parameters, and realizes the purpose of reducing the cogging torque by optimizing the parameters of stator tooth width, slot width and the number of stator slots.

3 Method to Reduce Cogging Torque

As the rotor tooth width of LSPMSM changes to θ_{ra} , the distribution map of $F^2(\theta)$ is shown in Fig. 4. So the amplitude of $F^2(\theta)$ is changed as.

$$F_1^2 = \frac{\theta_{rs}^2}{\theta_{ra}^2} F^2 \tag{13}$$

In addition, the Fourier decomposition coefficient $F^2(\theta)$ is changed as.

$$F_0 = \frac{(q_2 - 1)pF_1^2}{\pi} \theta_{ra} \tag{14}$$

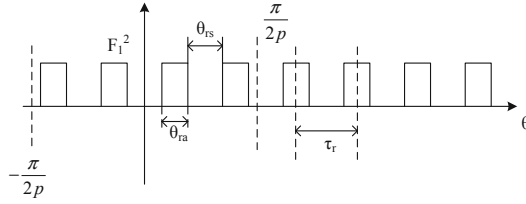


Fig. 4. Distribution of $F^2(\theta)$ as the rotor tooth is θ_{ra}

The cogging torque is related to $F_{nQ1}/2p$, and let Fourier decomposition coefficient is 0.

$$\sin \frac{t_0 nQ_1}{t_2 Q_2} \pi = 0 \quad (15)$$

$$\frac{t_0 nQ_1}{t_2 Q_2} \pi = k\pi, \quad k \text{ is an integer} \quad (16)$$

It can be obtained that when the rotor tooth width and the rotor tooth pitch meet $t_2/t_0 = nQ_2/kQ_1$, the cogging torque can be reduce effectively. Take the case of a 72 stator slot- 8 pole spoke-type LSPMSM, and the influence of rotor parameters on cogging torque is studied. In Table 1, the main parameters of the machine are listed.

Meanwhile, the comparison of cogging torque waveforms of LSPMSM with initial model and optimized model are shown in Fig. 5. Obviously, the cogging torque is reduced as the rotor tooth is 5° .

Table 1. Main parameters of prototype machine

Item	Value	Item	Value
Rated power/kW	30	Core material	BAT1500
PM material	N35EH	Air-gap length/mm	1
Pole	8	PM width/mm	48
Stator slot Q_1	72	PM thickness/mm	12
Outer diameter of stator /mm	400	Pressure coefficient	0.97
Outer diameter of rotor /mm	283.6	Rotor inner diameter /mm	85
Axial length/mm	225	Rated voltage/V	380

Change the rotor slots. According to the air-gap flux density Fourier decomposition, and the rotor slot will make the harmonic amplitude of the rotor MMF increases. In addition, the air-gap flux density harmonic content can be changed as the rotor slot number increases, and the cogging torque must change. In order to study the number of rotor slots is influenced on the cogging torque, and the FEA model is established with different rotor slots.

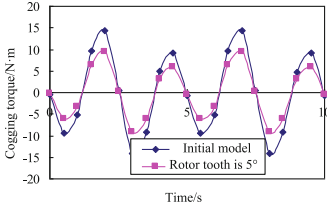


Fig. 5. Slot torque of different rotor tooth width

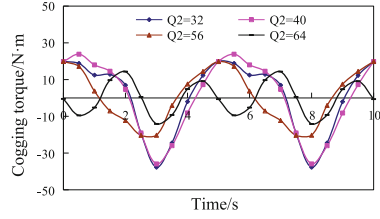


Fig. 6. Relationship between cogging torque and rotor slot number

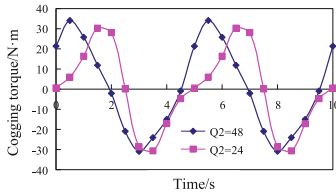


Fig. 7. Relationship between cogging torque and rotor slot number

Figure 6 and Fig. 7 shows the cogging torque versus number of rotor slot. It can be noted that the number of cycles and amplitude of cogging torque are changed with the number of rotor slots changes. The cogging torque of 32 rotor slot and 40 rotor slot is similar, and the cogging torque of 56 rotor slot is closed to 64 rotor slot. In order to further study the influence of rotor slot number on cogging torque, and the cogging torque of different rotor slots is shown in Table 2.

Table 2. Cogging torque with different rotor slot

Q2	Nq	Nq2p/Q2	COGGING TORQUE(N·m)
24	9	3	31
32	36	9	43
40	45	9	42
48	18	9	34
56	63	9	20
64	72	9	16

We could draw the following conclusions that: when the value of $Nq2p/Q2$ is larger, the amplitude of cogging torque is smaller. It is because of the value of $Nq2p/Q2$ is larger, and the flux density harmonic components of rotor tooth is lower.

Effect on the rotor tooth shape. The outer diameter of rotor is different from the inner diameter of stator when the shaped of rotor tooth is changed. There is an eccentric

distance between the rotor center and the stator center, and denoted as h_{px} , as shown in Fig. 8. It can be seen that the air-gap length is non-uniform, and the air-gap length changes with the change of rotor position. Therefore, the distribution of air-gap magnetic field along the circumference is changed, and the cogging torque is reduced.

The LSPMSM cogging torque versus eccentric distance are shown in Fig. 9. It can be seen that the cogging torque decreases with the increase of eccentric distance, and the amplitude of cogging torque from 9.5N·m reduce to 4.5N·m. However, when the eccentric distance reaches 15mm, the reduction of cogging torque is not obvious with the increase of eccentric distance. As a results, the eccentric distance is selected 15mm.

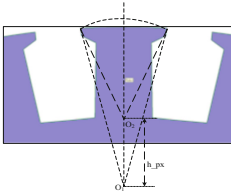


Fig. 8. The configuration of rotor tooth with eccentric

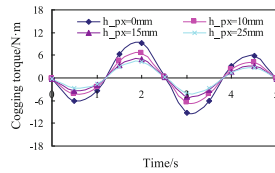


Fig. 9. The cogging torque versus eccentric distance

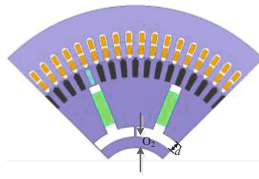


Fig. 10. Structure of magnetic bridge

Effect on the magnetic bridge size. The size of magnetic bridge can influence on the distribution of rotor magnetic field, so the cogging torque is effected on magnetic bridge size. The structure and size of magnetic bridge is shown in Fig. 10. The distance between magnetic bridge and shaft is defined as O_2 , and the magnetic bridge width is defined as d .

Figure 11 shows the cogging torque and rated torque versus distance magnetic bridge and shaft. It can be seen that the cogging torque decreases first and then increases with the increase of distance between magnetic bridge and shaft. However, the rated torque keep constant with the increase of distance between magnetic bridge and shaft. Because of the air-gap flux density keep constant as the volume of PM is equal. Figure 12 shows the cogging torque and rated torque versus magnetic bridge width. It can be noted that the cogging torque decrease obviously first and then reduces with the increases of magnetic bridge width, and the rated torque increases and then decreases with the increase of magnetic bridge width.

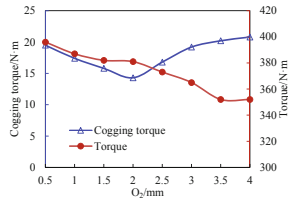
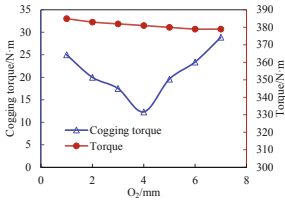


Fig. 11. The cogging torque versus eccentric distance

Fig. 12. The cogging torque versus eccentric distance

4 Performance of LSPMSM After Optimized

It can be seen from the above conclusion, and the cogging torque of LSPMSM can be weakened effectively for the rotor parameters are changed. However, the electromagnetic performance has been changed with the rotor parameters are changed. By using the time-step finite element method, the no-load back-EMF and rated electromagnetic torque of the prototype before and after optimization are calculated and compared, as shown in Table 3 and Table 4.

It can be noted that the amplitude of back-EMF no large change by adopting the measures of cogging torque reduction in this paper. In addition, the change of starting torque and starting-current of the prototype is also small. Therefore, the cogging torque reduction method in this paper can effectively weaken the cogging torque of the LSPMSMs, and will not have a great impact on the performance of the machine.

Table 3. Comparison of no-load performance of the prototype machine

Model	Back-EMF	THD	Cogging torque
Original Model	246.7 V	3.5%	16.2 N·m
Change rotor tooth	245.4 V	3.2%	10.5 N·m
Change rotor tooth shaped	235.6 V	2.7%	5.7 N·m
Unequal rotor tooth	237.2 V	3.0%	N·m

Table 4. Comparison of load performance of the prototype machine

Model	Stating-torque	Rated torque	Starting-current
Original Model	875 N·m	381 N·m	378 A
Change rotor tooth	889 N·m	376 N·m	387 A
Change rotor tooth shaped	905 N·m	372 N·m	399 A
Unequal rotor tooth	897 N·m	374 N·m	

5 Conclusions

LSPMSMs have been increased interest due to self-starting capability, high power factor and high efficiency. Cogging torque is a common problem to LSPMSMs, and it is one of the issues that should be paid attention to at the design stage. Meanwhile, LSPMSMs has rotor slots in the rotor core due to improve the self-starting capability, and the cogging torque will adversely the operation of LSPMSM. In order to comperhend the cogging torque of LSPMSM mechanism, and the analytical expression of the cogging torque with the changing the rotor tooth width, rotor slots and the rotor tooth shaped are deduced in this paper, then some conclusions can be obtained as follows:

- (1) The interior PM rotor is equivalent to the MMF generated by the surface PM can simplify the cogging torque analytical model of LSPMSM.
- (2) The number of rotor slots have influenced on the cogging torque of LSPMSM. When the larger $N_q 2p/Q_2$ is selected, the cogging torque of the LSPMSM can be reduced.
- (3) Selecting appropriate rotor tooth width can effectively weaken the cogging torque of LSPMSM.
- (4) The appropriate rotor eccentricity distance can further reduce the cogging torque of the LSPMSM.

References

1. Cheng, M., Hua, W., Zhang, G.: Overview of stator-permanent magnet brushless machines. *IEEE Trans. Industr. Electron.* **61**(8), 5087–5101 (2011)
2. Cheng, M., Zhang, G., Hua, W.: Overview of stator permanent magnet brushless machine systems and their key technologies. *Proc. CSEE* **34**(29), 5204–5220 (2014)
3. Liu, X.P., Zheng, A.H., Wang, CH.: 3-D Finite element analysis and experiment study of a stator-separated axial flux-switching hybrid excitation synchronous machine, *Transactions of china electro-technical society* **27** (10) 2012, 110–113
4. Hwang, S., Eom, J., Jung, Y., Lee, D., Kang, B.: Various design techniques to reduce cogging torque by controlling energy variation in permanent magnet motors. *IEEE Trans. Magn.* **37**(4), 2806–2809 (2001)
5. Yongping, L., Yong, L.: Tooth-slot cogging torque and noise analysis of permanent magnet motors. In: *Proceedings of the Fifth International Conference on Electrical Machines and Systems*, Shenyang, pp. 860–862 (2001)
6. Li, J.T., Liu, Z.J., Jabbar, M.A.: Design optimization for cogging torque minimization using response surface methodology. *IEEE Trans. Magn.* **40**(2), 1176–1179 (2004)
7. Bianchini, C., Immovilli, F., Lorenzani, E., et al.: Review of design solutions for internal permanent-magnet machines cogging torque reduction. *IEEE Trans. Magn.* **48**(10), 2685–2693 (2001)
8. Islam, J., SvechKarenko, D., Chin, R., et al.: Cogging torque and vibration analysis of a direct-driven PM wind generator with concentrated and distributed windings. In: *2012 15th International Conference on Electrical Machines and Systems*, Sapporo, pp. 1–6 (2012).
9. Xintong, J., Jingwei, X., Yong, L., et al.: Theoretical and simulation analysis of influences of stator tooth width on cogging torque of BLDC motors. *IEEE Trans. Magn.* **45**(10), 4601–4604 (2009)

10. Fei, W., Luk, P.C.K., Shen, J.: Torque analysis of permanent-magnet flux switching machines with rotor step skewing. *IEEE Transactions on Magnetics* 48(10), 2664–2673 (2012). <https://doi.org/10.1109/TMAG.2012.2198223>
11. Wang, D.H., Wang, X.H., Jung, S.Y.: Reduction on cogging torque in flux-switching permanent magnet machine by teeth notching schemes. *IEEE Trans. Magn.* **48**(11), 4228–4231 (2012). <https://doi.org/10.1109/TMAG.2012.2200237>
12. Hao, L., Lin, M.Y., Xu, D.: Cogging torque reduction in axial field flux-switching permanent magnet machines. *Trans. China Electro-Tech. Soc.* **30**(2), 21–26 (2015)
13. Hao, L., Lin, M.Y., Xu, D.: Cogging torque reduction of axial field flux-switching permanent magnet machine by adding magnetic bridge in stator tooth. *IEEE Trans. Appl. Supercond.* **24**(3), 503–506 (2014). <https://doi.org/10.1109/TASC.2014.2302911>